



**HAL**  
open science

## Parvalbumin gates chronic pain through the modulation of firing patterns in inhibitory neurons

Haoyi Qiu, Loïs S Miraucourt, Hugues Petitjean, Mengyi Xu, Catherine Theriault, Albena Davidova, Vanessa Soubeyre, Gaetan Poulen, Nicolas Lonjon, Florence Vachi-Lahaye, et al.

### ► To cite this version:

Haoyi Qiu, Loïs S Miraucourt, Hugues Petitjean, Mengyi Xu, Catherine Theriault, et al.. Parvalbumin gates chronic pain through the modulation of firing patterns in inhibitory neurons. Proceedings of the National Academy of Sciences of the United States of America, 2024, 121 (27), pp.e2403777121. 10.1073/pnas.2403777121 . hal-04626317

**HAL Id: hal-04626317**

**<https://hal.science/hal-04626317>**

Submitted on 26 Jun 2024

**HAL** is a multi-disciplinary open access archive for the deposit and dissemination of scientific research documents, whether they are published or not. The documents may come from teaching and research institutions in France or abroad, or from public or private research centers.

L'archive ouverte pluridisciplinaire **HAL**, est destinée au dépôt et à la diffusion de documents scientifiques de niveau recherche, publiés ou non, émanant des établissements d'enseignement et de recherche français ou étrangers, des laboratoires publics ou privés.



Distributed under a Creative Commons Attribution - NonCommercial - NoDerivatives 4.0 International License



# Parvalbumin gates chronic pain through the modulation of firing patterns in inhibitory neurons

Haoyi Qiu<sup>a,b</sup>, Lois S. Miracourt<sup>a,b</sup>, Hugues Petitjean<sup>a,b</sup> , Mengyi Xu<sup>a,b</sup>, Catherine Theriault<sup>a,b</sup>, Alben Davidova<sup>a,b</sup>, Vanessa Soubeyre<sup>c</sup>, Gaetan Poulen<sup>d</sup>, Nicolas Lonjon<sup>d</sup>, Florence Vachery-Lahaye<sup>d</sup>, Luc Bauchet<sup>c,d</sup> , Philipa Levesque-Damphousse<sup>e</sup> , Jennifer L. Estall<sup>e</sup> , Emmanuel Bourinet<sup>c</sup>, and Reza Sharif-Naeini<sup>a,b,1</sup>

Edited by Mark Nelson, University of Vermont, Burlington, VT; received February 22, 2024; accepted May 14, 2024

Spinal cord dorsal horn inhibition is critical to the processing of sensory inputs, and its impairment leads to mechanical allodynia. How this decreased inhibition occurs and whether its restoration alleviates allodynic pain are poorly understood. Here, we show that a critical step in the loss of inhibitory tone is the change in the firing pattern of inhibitory parvalbumin (PV)-expressing neurons (PVNs). Our results show that PV, a calcium-binding protein, controls the firing activity of PVNs by enabling them to sustain high-frequency tonic firing patterns. Upon nerve injury, PVNs transition to adaptive firing and decrease their PV expression. Interestingly, decreased PV is necessary and sufficient for the development of mechanical allodynia and the transition of PVNs to adaptive firing. This transition of the firing pattern is due to the recruitment of calcium-activated potassium (SK) channels, and blocking them during chronic pain restores normal tonic firing and alleviates chronic pain. Our findings indicate that PV is essential for controlling the firing pattern of PVNs and for preventing allodynia. Developing approaches to manipulate these mechanisms may lead to different strategies for chronic pain relief.

parvalbumin | dorsal horn | chronic pain

Chronic neuropathic pain is a debilitating disease that follows nerve injury and persists long after the injury has subsided (1). Spontaneous pain and mechanical allodynia, a painful response to an innocuous stimulus, are two hallmarks of neuropathic pain and are thought to be due in part to decreased inhibitory transmission at the level of the spinal cord (2–4). How this decreased inhibition occurs is not fully understood.

We and others have identified a subset of inhibitory neurons in the dorsal horn (DH) of the spinal cord that express the marker and calcium-binding protein parvalbumin (PV) and act as gate keepers that control the transfer of nociceptive (pain-like) information to the brain by preventing peripheral touch inputs from activating nociceptive circuits (5–10). Transiently silencing these PV neurons (PVNs) in naive mice produced mechanical allodynia, whereas activating them in mice with nerve injury attenuated the allodynia (5). Despite the critical role of these neurons in sensory processing and reports of their decreased output after nerve injury, the mechanisms underlying the reduced activity of PVNs remain unknown.

Here, we show that nerve injury causes a decrease in PV expression and PVNs display a drastic change in their firing patterns and transition from tonic to adaptive or initial burst firing. This transition occurs via the recruitment of calcium-activated potassium (SK) channels. These observations are associated with the development of mechanical allodynia. Importantly, we show a causal relationship between these events because decreasing PV expression transitions the firing pattern of PVNs from tonic to adaptive and leads to the development of mechanical allodynia in otherwise healthy mice. Finally, blocking SK channels in PVNs can restore tonic firing and alleviate mechanical allodynia in nerve-injured mice. Together, our results reveal a mechanism that explains the decreased inhibitory tone in the spinal DH after nerve injury, which may be amenable to therapeutic strategies aimed at alleviating chronic pain.

## Results

**PVN Firing Activity and PV Expression Are Disrupted after Nerve Injury.** We showed previously that PVNs function as modality-specific filters of sensory inputs in the DH. Silencing their activity in naive mice induces mechanical allodynia. On the other hand, activating them in a mouse model of neuropathic pain alleviates mechanical allodynia (8). After nerve injury, there is a loss of DH inhibitory tone driven partly by a decrease

## Significance

The processing of touch and pain inputs through the spinal cord relies on a finely tuned network of interneurons. During chronic pain, the output of spinal inhibitory neurons is reduced through mechanisms that have yet to be fully understood. Among these are inhibitory neurons with a characteristic high firing frequency. Our work demonstrates that during chronic pain, these neurons modify their firing patterns, and this change is responsible for the development of chronic pain. Importantly, we show that restoring the high-frequency firing pattern of these inhibitory neurons can attenuate chronic pain.

Author affiliations: <sup>a</sup>Department of Physiology, McGill University, Montreal, QC H3G 1Y6, Canada; <sup>b</sup>Alan Edwards Center for Research on Pain, McGill University, Montreal, QC H3A 2B4, Canada; <sup>c</sup>Institute of Functional Genomics, Montpellier University, CNRS, INSERM, Montpellier 34000, France; <sup>d</sup>Department of Neurosurgery, Gui de Chauliac Hospital, and Donation and Transplantation Coordination Unit, Montpellier University Medical Center, Montpellier 34295, France; and <sup>e</sup>Institut de Recherches Cliniques de Montréal, Montreal, QC H2W 1R7, Canada

Author contributions: H.Q. and R.S.-N. designed research; H.Q., L.S.M., H.P., M.X., C.T., A.D., V.S., G.P., N.L., F.V.-L., L.B., V.S., and E.B. performed research; P.L.-D. and J.L.E. contributed new reagents/analytic tools; H.Q., L.S.M., M.X., and E.B. analyzed data; R.S.-N. secured funding for the research; and H.Q. and R.S.-N. wrote the paper.

The authors declare no competing interest.

This article is a PNAS Direct Submission.

Copyright © 2024 the Author(s). Published by PNAS. This open access article is distributed under [Creative Commons Attribution-NonCommercial-NoDerivatives License 4.0 \(CC BY-NC-ND\)](https://creativecommons.org/licenses/by-nc-nd/4.0/).

<sup>1</sup>To whom correspondence may be addressed. Email: reza.sharif@mcgill.ca.

This article contains supporting information online at <https://www.pnas.org/lookup/suppl/doi:10.1073/pnas.2403777121/-DCSupplemental>.

Published June 25, 2024.

in the function, but not in the number of PVNs (8, 9). We hypothesized that this decreased function could be the result of decreased appositions onto their postsynaptic targets, reduced excitatory drive from A $\beta$  fibers, or altered electrical activity of PVNs. We therefore examined the electrical properties of PVNs after nerve injury induced by chronic constriction to the sciatic nerve (CCI). This was performed in PV<sup>cre</sup> mice crossed to the Ai14 reporter line, hereafter referred to as PV<sup>cre</sup>;tdTomato mice, which specifically labels a portion of DH PVNs (SI Appendix, Fig. S1A). When examined whether at 4 wk post-CCI, a time point when mice display significant mechanical allodynia (SI Appendix, Fig. S1B), PVNs in both males and females undergo a decrease in excitability (Fig. 1 A–D). Our results demonstrate that these neurons not only decrease their firing activity in response to current injections, but they seem to undergo a change in firing pattern where they display frequency adaptation and

can no longer sustain high-frequency firing (Fig. 1 A–D and SI Appendix, Fig. S2). However, we failed to observe any change in their resting membrane potential after nerve injury (SI Appendix, Fig. S2C). We found no significant differences in the action potential threshold (SI Appendix, Fig. S2 F and I), indicating overall excitable membrane properties remain unaffected by the injury. To examine the time course during which these changes in firing activity take place, we compared the firing patterns of PVNs from naive (0 d) and CCI mice 2, 7, and 28 d postinjury (Fig. 1 E and F). Our results show a gradual decrease in spike count and spiking duration occurring as early as 7 d post-CCI and becoming significant by day 28 post-CCI (Fig. 1E and SI Appendix, Fig. S3 A and B). However, the proportion of PVNs displaying adaptive firing increased within 2 d post-CCI and continued to increase until day 28 (Fig. 1F). There were no significant differences in spike threshold or resting membrane potential in any of the four

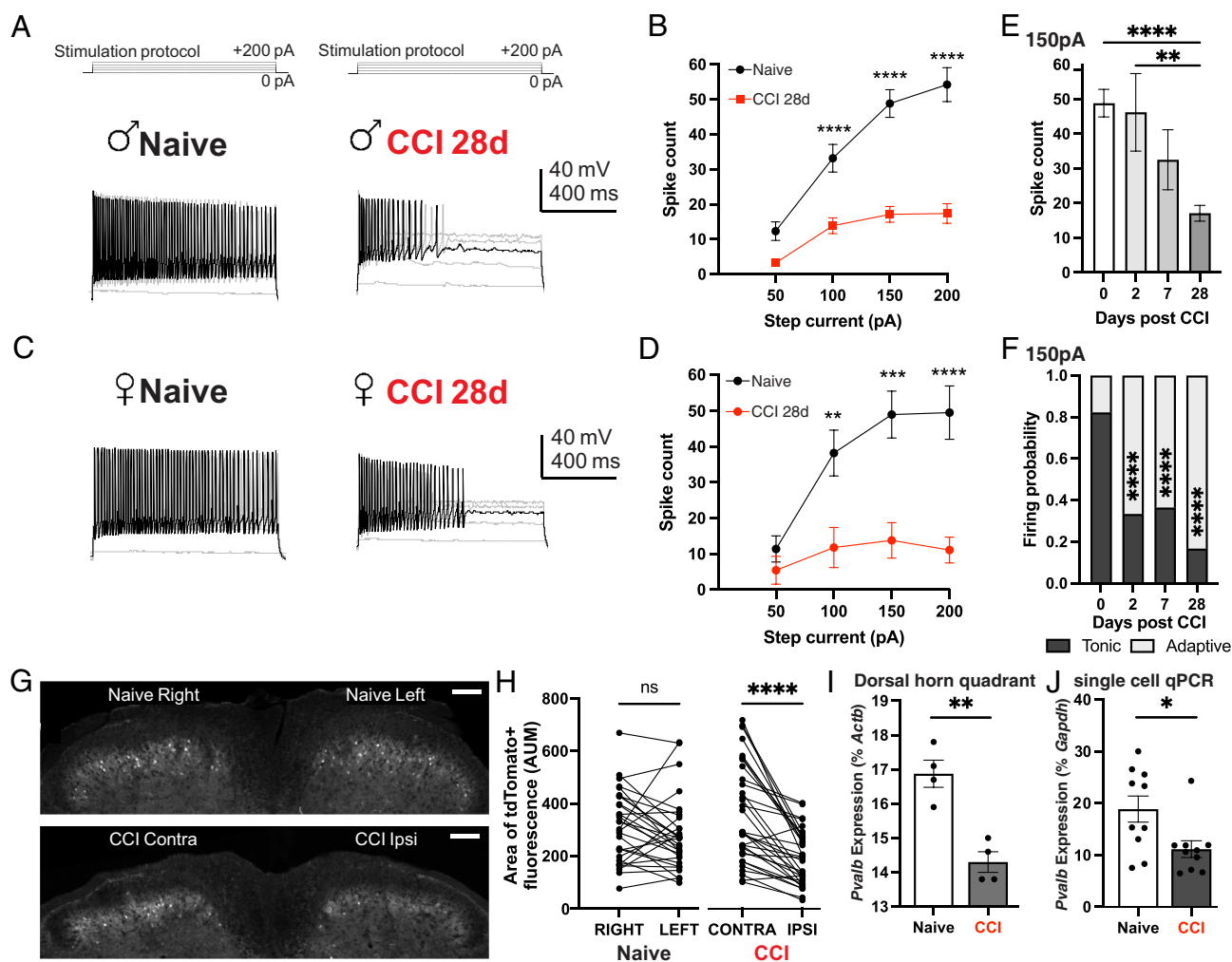


**Fig. 1.** PVN firing activity and PV expression are disrupted after nerve injury. (A) Whole-cell current-clamp representative traces of PVN response to step current injections in the lumbar DH of naive (Left) and 28 d post-nerve-injury (CCI 28 d) (Right) male mice. The same stimulation protocol is used for all subsequent electrophysiology traces unless otherwise stated. (B) Spike count (mean  $\pm$  SEM) of PVN response to step current injections in naive and CCI 28 d mice ( $n = 28$  cells from nine naive mice and  $n = 30$  cells from 16 CCI mice) \*\*\*\* $P$ -value  $< 0.0001$ , Two-way ANOVA, Šidák's multiple comparisons test. (C and D) Same as (A and B) in female mice. ( $n = 13$  cells from four naive mice and  $n = 9$  cells from 4 CCI mice.) \*\* $P$ -value = 0.0093, \*\*\* $P$ -value = 0.0003, and \*\*\*\* $P$ -value  $< 0.0001$ , two-way ANOVA, Šidák's multiple comparisons test. (E) Spike count (mean  $\pm$  SEM) of PVN response to a 150 pA step current injection in naive, 2 d, 7 d, and 28 d CCI mice ( $n = 28$  cells from nine naive mice,  $n = 9$  cells from 4 CCI 4 d mice,  $n = 11$  from 3 CCI 7 d mice, and  $n = 30$  cells from 16 CCI 28 d mice) \*\*\* $P$ -value = 0.0002 and \*\*\*\* $P$ -value  $< 0.0001$ , one-way ANOVA, Tukey's multiple comparisons test. (F) Percentage of tonic firing (dark bar) and adaptive firing (light bar) cells at 150 pA step current injection in naive, 2 d, 7 d, and 28 d CCI male mice. \*\*\*\* $P$ -value  $< 0.001$ , contingency test with Fisher's exact probability test compares each time point with naive. (G) Pvalb promoter-driven tdTomato fluorescence in transverse DH sections of naive and CCI 28 d Pvalb-tdTomato male mice. (Scale bar, 100  $\mu$ m.) (H) Reduced area of tdTomato-positive cells per spinal cord section ( $n = 33$  sections in 3 CCI mice) on the ipsilateral side in CCI male mice. \*\*\*\* $P$ -value  $< 0.0001$ , paired  $t$  test. No changes were observed in the area of tdTomato-positive cells in naive mice ( $n = 30$  sections in three naive mice). (I) Mean ( $\pm$ SEM) Pvalb expression relative to  $\beta$ -actin in the dorsal ipsilateral quadrant of naive and CCI 28d mice ( $n = 4$  mice per group). Results were normalized to *Actb* based on SI Appendix, Table S2. \*\* $P$ -value = 0.0021, unpaired  $t$  test. (J) Single-cell qPCR of Pvalb expression with respect to *Gapdh* in PVNs from naive and CCI 28 d mice ( $n = 13$  cells from three naive mice and  $n = 10$  cells from 3 CCI mice), \* $P$ -value = 0.049, unpaired  $t$  test.

time points (*SI Appendix, Fig. S3 C and D*). Thus, we decided to use the 28-d time point for the remainder of the experiments in our study. Our data indicate that after nerve injury, PVNs change their firing pattern from tonic to adaptive, which likely causes a decrease in their inhibitory output.

Such hypofunction of PVNs is reminiscent of the pathology observed in autism models, in which an increase in the ratio of excitation vs. inhibition is often observed (11–16). In these models, deficits relating to PVNs have been reported to result from reduction in PV protein expression, number of PV-expressing interneurons, or reduction in the fast-spiking behavior of the neurons. We previously reported that peripheral nerve injury did not affect the number of PVNs in the DH of the spinal cord (5). We therefore examined whether PV expression was affected by nerve injury. To examine whether nerve injury leads to a change in PV expression, we used a BAC transgenic mouse in which the PV promoter drives the expression of tdTomato (Pvalb-tdTomato mice) (17). We focused our analysis on PVNs located in the spinal segment affected by the nerve injury, evident by the increased microglia proliferation (18) (*SI Appendix, Fig. S1 C and D*). The expression of tdTomato is distributed throughout the soma and processes of these PVNs. Therefore, in a region of interest encompassing lamina IIi and III, we quantified in a blind fashion the area of tdTomato fluorescence. Our results show that in CCI mice, this region of the DH displays a significantly lower area of tdTomato fluorescence ipsilateral to the injury compared to the contralateral side (Fig. 1 *G and H*). These findings were supported by real time (RT)-qPCR experiments performed on ipsilateral dorsal quadrants (Fig. 1*I*) and on single-cell RT-qPCR (Fig. 1*J*) of CCI and naive mice, indicating a decrease in *Pvalb* mRNA.

Our results show that 4 wk after peripheral nerve injury, PVNs have significantly less PV expression. Since PV is one of the highest expressed calcium buffers in PVNs (19), we hypothesized that its downregulation would impact the cell's calcium handling capacity and calcium-dependent conductances, eventually changing the neurons' firing pattern and their inhibitory output. However, although the changes in behavior and protein expression are both observed after nerve injury, whether decreased PV is sufficient to induce mechanical allodynia remains to be determined.

**PV Expression Is Sufficient and Necessary for Preventing Mechanical Allodynia.** Nerve injury recruits several inflammatory processes in the DH, making it difficult to ascribe a role for the decrease in PV expression to the development of mechanical allodynia. Therefore, we examined whether deleting PV in naive mice would be enough to elicit the development of mechanical allodynia. We assessed the sensitivity to thermal and mechanical stimuli 1) in PV global knockout (PV KO) and wild-type (PV WT) mice (Fig. 2 *A and B*) and 2) in adult Pvalb-tdTomato mice with reduced expression of spinal PV (Fig. 2*C* and *SI Appendix, Fig. S4 A and B*). Compared to PV WT mice, PV KO mice displayed similar heat sensitivity, but their mechanical pain (nocifensive) threshold was significantly lower, indicating mechanical allodynia (Fig. 2 *A and B*). Next, naive Pvalb-tdTomato mice were intraspinally injected with lentiviruses containing shRNA molecules against PV (shPV) or control nontargeting (NT) sequences. Lentiviral vectors were chosen in this experiment because of the stable expression despite the delay required to observe their effect (20). Our results indicated that adult mice injected with the shPV lentivirus gradually developed mechanical allodynia, but not those injected with the NT lentivirus (Fig. 2*C* and *SI Appendix, Fig. S4D*). This hypersensitivity was modality specific for mechanical inputs because thermal sensitivity was unaffected (*SI Appendix, Fig. S4C*). These results indicate that a direct reduction in PV expression

alone is enough to induce mechanical allodynia in a healthy mouse similar to that seen after nerve injury and after silencing PVNs (8).

We postulated that the mechanical allodynia induced by decreasing PV is through the disinhibition of the postsynaptic targets of PVNs. Blocking the activity of these targets should therefore alleviate the allodynia induced by PVN hypofunction. We and others have demonstrated that one of the targets of PVNs in the DH are PKC $\gamma$ -expressing excitatory neurons (PKC $\gamma$  neurons) (5, 6, 21). To examine the proportion of PKC $\gamma$  neurons contacted by PVNs, we used a Cre-dependent anterograde transsynaptic tracer—wheat germ agglutinin (WGA) (22–24)—packaged in an AAV vector and injected in PV<sup>Cre</sup>;tdTom mice (Fig. 2*D*). Under these conditions, PVNs were the source of WGA production and transferred it to their postsynaptic targets. When examined 2 wk after virus injection, immunohistochemistry experiments revealed the presence of WGA in several non-PVNs, 17.6% of which were PKC $\gamma$  neurons (Fig. 2*E*). Importantly, nearly 80% of WGA-IR neurons were PKC $\gamma$  negative, indicating that PVNs have several other targets in the DH, including the recently reported vertical cells (6). It was shown that the inhibitory output of PVNs onto PKC $\gamma$  neurons was significantly lower in nerve-injured mice (21), further supporting the notion of a disinhibition of postsynaptic targets. In these excitatory neurons, the activity of the PKC $\gamma$  enzyme was shown to be central to their role in mechanical allodynia (5, 25, 26). To examine whether a disinhibition of PKC $\gamma$  neurons was driving the mechanical allodynia elicited by the downregulation of PV, we administered an intrathecal injection of the PKC $\gamma$  blocker  $\gamma$ V5-3 (27) (or the control TAT peptide) 8 wk after shPV lentivirus injection. Our results revealed that inhibiting PKC $\gamma$  in these mice significantly alleviated their mechanical allodynia (Fig. 2*F*). Taken together, our results show that reducing PV expression in an otherwise healthy mouse precipitates a mechanical allodynia akin to nerve injury, which is mediated in part by the disinhibition of PKC $\gamma$  neurons.

Nerve injury is associated with the activation of several spinal inflammatory pathways (28–30), some of which may presumably converge on mechanisms regulating PV expression. Therefore, we sought to identify endogenous processes controlling PV expression in the DH. In the cerebrum, one reported regulatory pathway controlling PV promoter activity is through a transcriptional coactivator named peroxisome proliferator-activated receptor- $\gamma$  coactivator (PGC)-1 $\alpha$ , referred to as PGC-1 $\alpha$  (31, 32). The expression of this coactivator is decreased by the TNF $\alpha$  pathway (33, 34), which is activated after nerve injury (35). Thus, we first examined whether PGC-1 $\alpha$  is expressed in DH PVNs. Our fluorescence in situ hybridization (ISH) results revealed that 80% of neurons that coexpress *Pvalb* and *Ppargc1a* (PGC-1 $\alpha$ ) also express *Slc32a1* (VGAT) and are classified as inhibitory (*SI Appendix, Fig. S5 A and B*). Among the inhibitory PVNs (that coexpress *Pvalb* and *Slc32a1*), 66% also expressed *Ppargc1a* above the detection threshold (*SI Appendix, Fig. S5C*). These data indicate that the majority of DH inhibitory PVNs coexpress PGC-1 $\alpha$  and that most PGC-1 $\alpha$  positive PVNs contain inhibitory markers. We then investigated whether PGC-1 $\alpha$  regulates PV expression in DH PVNs. We decreased PGC-1 $\alpha$  expression with an intraspinal injection of an adenovirus carrying an shRNA against PGC-1 $\alpha$  (shPGC-1 $\alpha$ ) in Pvalb-tdTomato mice, in which tdTomato expression is controlled by the PV promoter. Our results indicated that mice treated with shPGC-1 $\alpha$  showed a decrease in tdTomato+ cells ipsilateral to the injected side compared to the control virus (shControl) (Fig. 2 *G and H*) and compared to a spinal segment outside the injection site (*SI Appendix, Fig. S5D*). These results indicate that knocking down PGC-1 $\alpha$  leads to a decrease in PV expression. Furthermore, we tested the effect of this knockdown on the mice mechanical sensitivity and observed the presence of mechanical

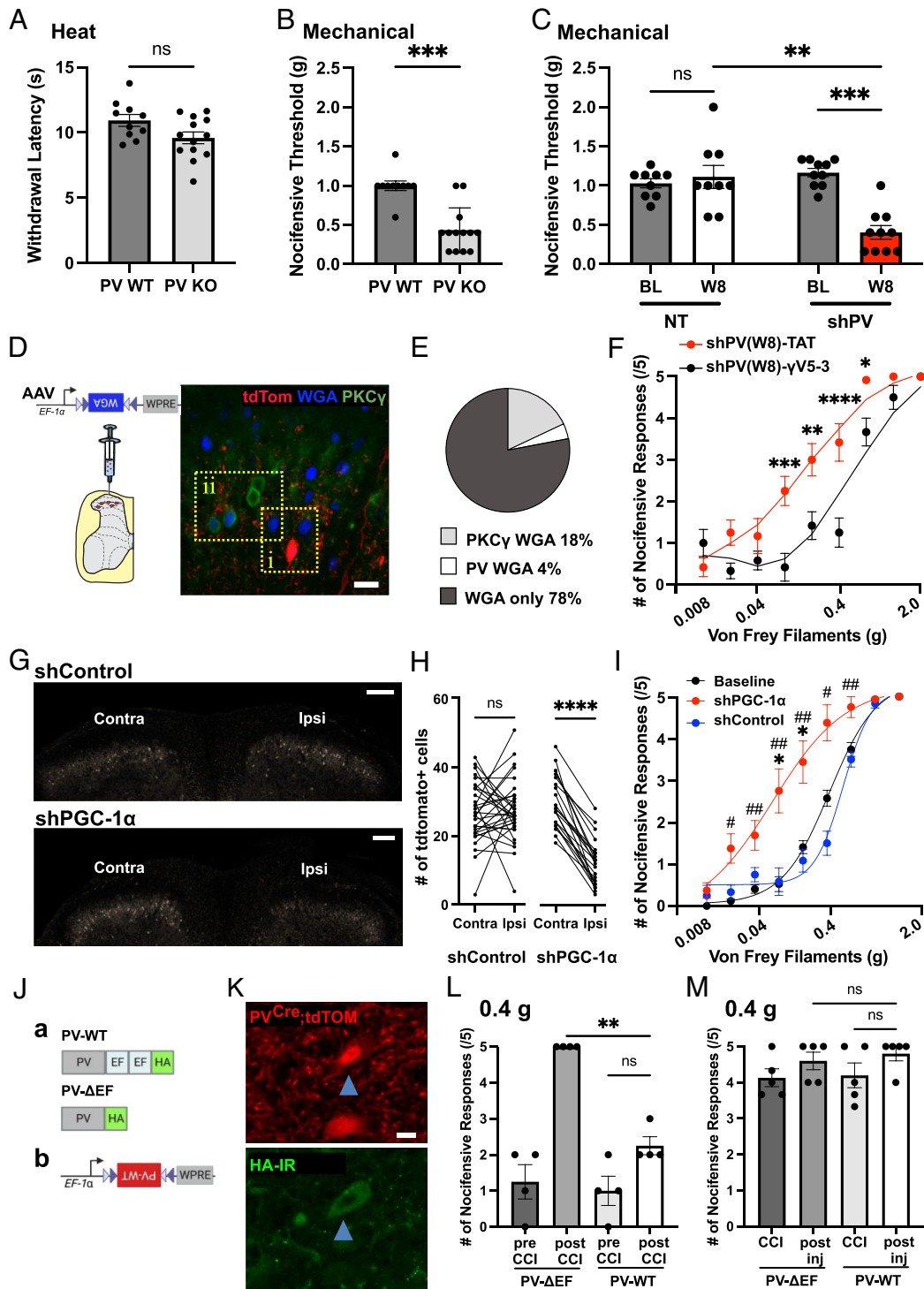


**Fig. 2.** PV expression is sufficient and necessary for preventing mechanical allodynia. (A and B) Paw withdrawal latency to heat (A) and nocifensive threshold to mechanical stimuli (B) of PV knockout (PV KO,  $n = 13$ ) mice (light gray bar) and PV wild-type (PV WT,  $n = 11$ ) mice (dark gray bar). ns, not statistically significant, unpaired  $t$  test. \*\*\* $P$ -value  $< 0.001$ , unpaired  $t$  test. (C) Intraspinal delivery of a lentivirus carrying PV shRNA ( $n = 10$  mice) produces mechanical allodynia 8 wk postinjection (W8) compared to baseline (BL). Mice receiving scrambled shRNA ( $n = 9$ ) are unaffected. Two-way ANOVA, Sidak's multiple comparisons test. \*\* $P$ -value = 0.0088 and \*\*\* $P$ -value  $< 0.001$ . (D and E) Spinal injection of AAV2/2-EF1α-DIO-WGA, allows for the expression of WGA in tdTomato+ PVNs (red, box i) (10/284 neurons), and their postsynaptic neurons (blue) which colocalize with PKCγ-expressing neurons (green, box ii) (50/284), or unidentified neurons (224/284). (Scale bar, 10  $\mu$ m.)  $n = 11$  sections from three mice. (F) Mean ( $\pm$ SEM) nocifensive responses in PV shRNA mice (shPV-W8) 20 min after an intrathecal injection of the control TAT peptide (red,  $n = 6$ ) or PKCγ enzyme inhibitor, γV5-3 (100 pmol) (black,  $n = 6$ ). \* $P$ -value = 0.0297, \*\* $P$ -value = 0.0022, \*\*\* $P$ -value = 0.0002, and \*\*\*\* $P$ -value  $< 0.0001$ , two-way ANOVA, Tukey's multiple comparisons test. (G and H) DH images (G) and quantification of tdTomato-positive cells (H) in Pvalb-tdTomato mice intraspinaly injected with shPGC-1α (Bottom) or shControl adenovirus (Top) 4-d postinjection. (Scale bar, 100  $\mu$ m.) ( $n = 32$  sections from three shControl-treated mice and  $n = 22$  section from shPGC-1α-treated mice) \*\*\*\* $P$ -value  $< 0.0001$  paired  $t$  test. (I) Same as (F) in shPGC-1α-injected mice ( $n = 8$ ) 4-d postinjection (red) compared to shControl (blue,  $n = 6$ ), and baseline (black,  $n = 14$ ). Two-way ANOVA, Tukey's multiple comparisons test, #, # compares shPGC-1α to shControl and baseline, respectively. (J) AAV viral construct to overexpress PV in PVNs. (K) Neuroanatomical section of DH PV<sup>Cre</sup>;tdTom neurons (red, Top) expressing the PV-WT sequence (blue arrowhead) visualized by a HA-tag (HA-IR; green, Bottom). (Scale bar, 10  $\mu$ m.) (L) Mean ( $\pm$ SEM) of the number of nocifensive responses out of five von Frey filament stimulations (0.4 g) in mice injected with either the PV-ΔEF or the PV-WT sequence before nerve injury (CCI) \*\* $P$ -value = 0.0014, two-way ANOVA, Tukey's multiple comparisons test. ( $n = 4$  PV-WT and  $n = 4$  PV-ΔEF). (M) Same as (L) in mice injected with the PV-ΔEF or the PV-WT sequence after CCI. n.s. nonstatistically significant, two-way ANOVA, Tukey's multiple comparisons test. ( $n = 5$  PV-WT and  $n = 5$  PV-ΔEF).

allodynia in shPGC-1 $\alpha$ - but not shControl-injected mice (Fig. 2*L*). Our data suggest that a decrease in PGC-1 $\alpha$  activity may be responsible for the decrease in PV expression after nerve injury.

Our results demonstrate that nerve injury produces a decrease in PV expression and that this decrease is sufficient to the development of mechanical allodynia in otherwise healthy mice. However, it is unknown whether this decreased PV expression seen after nerve injury is necessary for the development of mechanical allodynia. Thus, we examined whether nerve injury-induced mechanical allodynia would be prevented or alleviated by restoring PV expression. This expression was exogenously restored with a virus encoding a Cre-dependent HA-tagged PV (termed PV-WT) or an inactive control lacking Ca<sup>2+</sup> binding domains (termed PV- $\Delta$ EF) (Fig. 2*J* and *K*). The specificity of these approaches was validated in vitro (*SI Appendix*, Fig. S4*E*). When we increased PV expression 2 wk before nerve injury, we observed (2 wk after nerve injury) that PV-WT injected mice developed significantly less mechanical allodynia compared to PV- $\Delta$ EF injected mice (Fig. 2*L*). However, increasing PV expression 2 wk after nerve injury did not alleviate the mechanical allodynia (Fig. 2*M*). These findings indicate that increasing PV expression can prevent, but not alleviate, the development of mechanical allodynia after nerve injury. Taken together, our results demonstrate a relation between PV expression and the development of mechanical allodynia. In this relation, both a direct and indirect decrease in PV expression induces mechanical allodynia (Fig. 2*A–C* and *G–I*, respectively), and inhibiting the targets of PVNs or preventing PV downregulation attenuates the development of mechanical allodynia (Fig. 2*F* and *I*, respectively). Whether this relation involves a change in the firing properties of PVNs remains unclear.

**PV Expression Permits the Tonic Firing Pattern of PVNs.** We examined whether the same decrease in PV expression that caused mechanical allodynia in otherwise healthy animals would also be associated with a perturbation in the firing pattern of PVNs, similar to what is observed after nerve injury. To visually identify PVNs that would take up the shRNA against PV, we developed a mouse strain (PV<sup>Cre</sup>;RCF tdTOM mice) and used an AAV vector containing a Cre-dependent FLPo recombinase and a shRNA against PV (shPvalb). In these mice, PVNs that took up the virus (control or shPvalb) would express FLPo and be visually identifiable for spinal cord slice electrophysiology through the expression of TdTomato (Fig. 3*A*) (*Materials and Methods*). We verified the development of mechanical allodynia and the decrease in PV-immunoreactivity of the tdTomato+ cells in mice that received shPvalb compared to nontargeting shRNA (NT) 10 d after injection (Fig. 3*B–E*).

Our results demonstrated that decreasing PV expression in DH PVNs changes their firing pattern from tonic to adaptive (Fig. 3*F–H*), despite having no effect on the resting membrane potential or spike threshold (*SI Appendix*, Table S1, unpaired *t* test). We next examined whether the PV-mediated control of tonic firing activity extended to PVNs in other CNS regions. We injected shPvalb in the hippocampus of PV<sup>Cre</sup>;RCF tdTOM mice, where a population of tonic firing inhibitory PVNs has been described (36). Our results indicated that reducing PV in these neurons also caused a transition in their firing activity from tonic to adaptive, strikingly similar to that observed in the DH (Fig. 3*I–K*). The resting membrane potential and spike threshold were not affected by the decrease in PV (*SI Appendix*, Table S1, unpaired *t* test). These findings indicate that the PV control of the tonic firing pattern is a mechanism conserved in the CNS. Taken together, our results indicate that a decrease in PV alone is sufficient to trigger the development of mechanical allodynia and change the firing pattern of PVNs.

**PVNs Express Functional SK Channels Responsible for Frequency Adaptation and Mechanical Allodynia after Nerve Injury.** Despite the impact of PV on the firing pattern of PVNs, the ionic mechanisms underlying these neuronal effects remain unknown. This transition could be the result of a decrease in conductances that enable tonic firing, such as HCN channels (37, 38). However, we found that blocking HCN channels in PVNs with the pan-selective antagonist ZD7288 (39, 40) did not decrease their firing pattern (*SI Appendix*, Fig. S6). PV is a calcium-binding protein, whose binding kinetics can be reproduced by synthetic buffers such as EGTA (41, 42). We hypothesized that if the effect of decreasing PV is due to impaired calcium buffering, then introducing a higher concentration of EGTA (*Materials and Methods*) in the recording electrode when recording from PVNs of nerve-injured mice should rescue their firing pattern. As expected, our results showed that after 2 mM EGTA dialyzed inside the cell (15 min), PVNs transitioned their firing pattern from adaptive to tonic firing. This transition was not observed in the 0.1 mM EGTA group which was used for all other recordings (Fig. 4*A–C* and *SI Appendix*, Table S2). These observations indicate that the ionic mechanisms affected by changes in PV expression are calcium dependent and contribute to neuronal firing patterns. Thus, calcium-activated potassium channels, like SK channels, represent likely candidates (43, 44).

We hypothesized that the nerve injury-induced decrease in PV expression may reduce the ability of PVNs to chelate action potential-driven calcium accumulation, thus enabling the activation of SK channels and the shift from tonic to adaptive firing patterns. To determine whether PVNs express SK channel isoforms (*Kcnn1–4*), we used RT-qPCR on spinal dorsal quadrants and found that all four isoforms were present, although *Kcnn2* and *Kcnn3* were expressed at higher levels [29.67  $\pm$  1.9% *Kcnn1*, 119.2  $\pm$  7.0% *Kcnn2*, 87.0  $\pm$  2.8% *Kcnn3*, 1.33  $\pm$  0.2% *Kcnn4* normalized to the house-keeping gene, TATA-binding protein (*Tbp*), *n* = 3 mice]. This observation is supported by a DH single cell RNA-sequencing database (19), reporting high expression of *Kcnn2* and low expression of *Kcnn3* in the same inhibitory neuronal cluster as *Pvalb* (cluster 14). We further confirmed the expression of these channel isoforms by ISH and demonstrated that *Kcnn2* is the predominant isoform of SK channels in DH inhibitory PVNs (Fig. 4*D* and *E*). To determine whether these channels play a functional role, we examined the effect of their activation on the tonic firing activity of PVNs. Our results demonstrated that the application of the SK channel agonist, 1-EBIO, can impose frequency adaptation in tonic firing DH PVNs (Fig. 4*F* and *G*). Importantly, our results demonstrate that the control of SK channels on the firing pattern of PVNs extends beyond the spinal cord and can also be observed in the hippocampus (*SI Appendix*, Fig. S7*A* and *B*).

Given the close resemblance in the firing patterns of DH PVNs from nerve-injured mice to PVNs from naive mice treated with 1-EBIO, we hypothesized that SK channels may become functionally active in PVNs after nerve injury. In that scenario, the decrease in PV expression after nerve injury enables the accumulation of intracellular calcium, which activates SK channels to produce frequency adaptation. Consequently, inhibiting these channels in PVNs of nerve-injured mice should reverse their adaptive behavior and restore tonic firing pattern. Indeed, our results demonstrate that bath application of the pan-selective SK channel blocker apamin (45) partially restored the tonic firing activity of DH PVNs in nerve-injured mice (Fig. 4*H* and *I*). Because of the predominant expression of *Kcnn2* in these inhibitory PVNs, we examined whether these channels contribute to the adaptive firing pattern. As expected, blocking SK2 channels with the specific antagonist Lei-Dab7 (46) restored tonic firing in PVNs from CCI animals (Fig. 4*J*). When

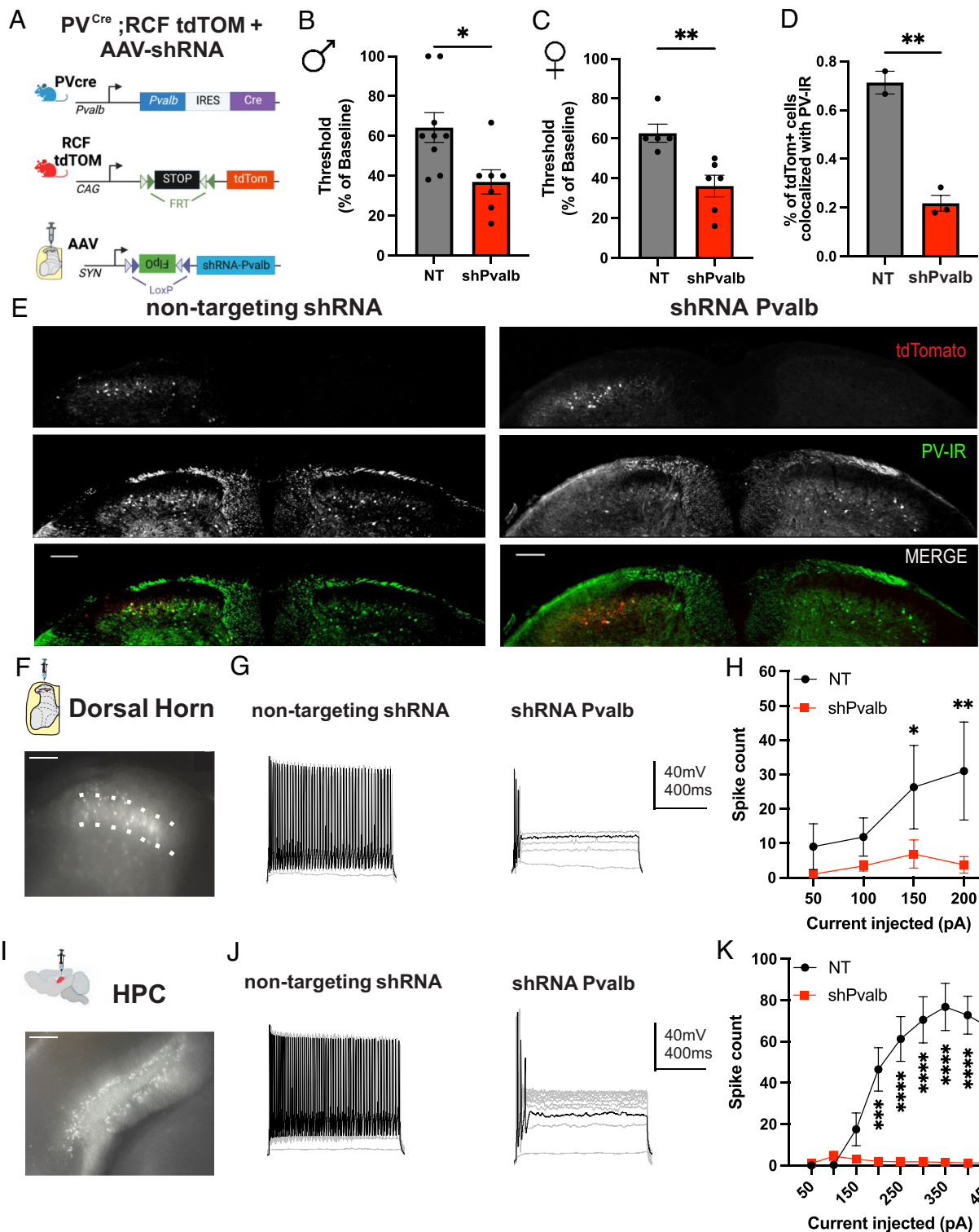


**Fig. 3.** PV controls tonic firing of PVNs in the DH and hippocampus. (A) Schematic diagram of the technique to visualize shPvalb expressing PVNs for spinal cord slice electrophysiology (*Materials and Methods*). (B) Mean ( $\pm$ SEM) mechanically evoked response threshold as a percent of baseline in PV<sup>Cre</sup>;RCF tdTomato male mice injected with shRNA-Pvalb ( $36.95 \pm 6.0\%$ ,  $n = 7$  mice, red, shPvalb) or nontargeting ( $64.23 \pm 7.5\%$ ,  $n = 9$  mice, gray, NT). \* $P$ -value = 0.0166, unpaired  $t$  test. (C) Same as in (B) in female mice ( $36.11 \pm 5.4\%$ ,  $n = 6$  shPvalb) ( $62.67 \pm 4.5\%$ ,  $n = 5$  NT) \*\* $P$ -value = 0.0053, unpaired  $t$  test. (D and E) Transverse DH sections of PV<sup>Cre</sup>;RCF tdTomato mice injected with either NT (Left) or shPvalb (Right) (E). Anti-PV staining (green) showed that  $21.79 \pm 3.3\%$  of tdTomato+ cells were PV-immunoreactivity (IR)-positive in the shPvalb-injected mice ( $n = 21$  sections from three mice, red), whereas  $71.33 \pm 4.7\%$  of tdTomato-positive cells were PV-IR-positive in the NT control ( $n = 13$  sections from two mice, gray). \*\* $P$ -value = 0.0028, unpaired  $t$  test. (Scale bar, 100  $\mu$ m.) (F) Epifluorescence image of a spinal cord slice from a shPvalb injected PV<sup>Cre</sup>;RCF tdTomato mouse showing tdTomato-positive used for targeted electrophysiology recordings. (Scale bar, 100  $\mu$ m.) (G and H) Whole-cell current clamp representative traces (G) and mean  $\pm$  SEM of PVNs in response to step current injections (H) recorded in the DH of NT- (G, Left) and shPvalb-injected male and female mice (G, Right). ( $n = 6$  cells from 4 NT-injected mice and  $n = 7$  from 3 shPvalb-injected mice). \* $P$ -value = 0.0236 and \*\* $P$ -value = 0.0025, uncorrected Fisher's LSD. (I) Same as (F) in the hippocampus (HPC) of the shPvalb-injected PV<sup>Cre</sup>;RCF tdTomato mouse. (Scale bar, 100  $\mu$ m.) (J and K) Same as (G and H) in the hippocampus PVNs of NT- (J, Right) and shPvalb-injected mice (J, Right). ( $n = 4$  cells from an NT-injected mouse and  $n = 4$  cells from a shPvalb-injected mouse). \*\*\* $P$ -value = 0.004 and \*\*\*\* $P$ -value < 0.0001, two-way ANOVA, Sidák's multiple comparisons test.

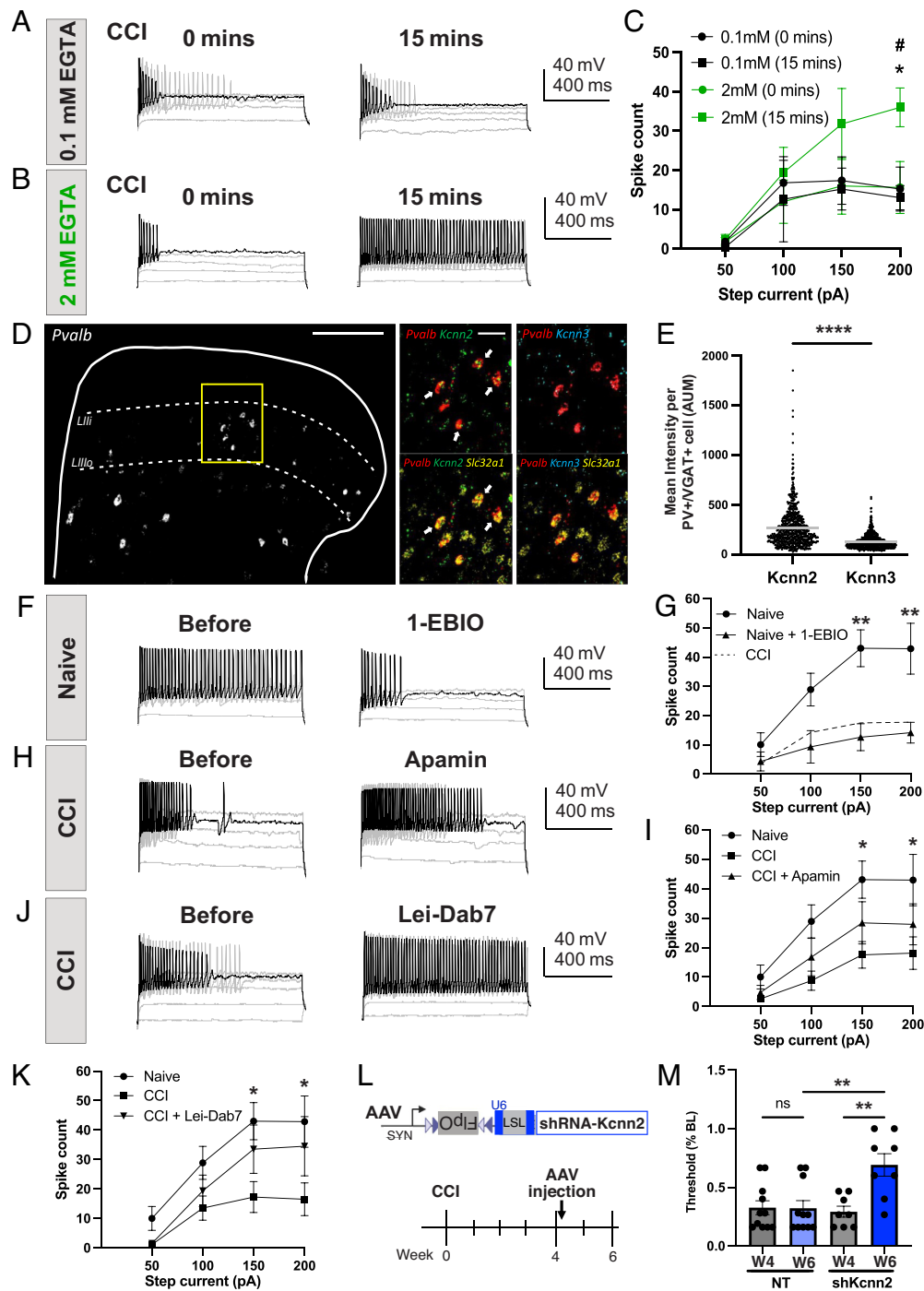


**Fig. 4.** Blocking SK channels of PVNs after nerve injury alleviates mechanical allodynia. (A–C) Whole-cell current clamp representative traces and mean  $\pm$  SEM of PVNs spike count (C) in response to increasing step current injections recorded in the lumbar DH spinal cord of CCI male mice 0 min (Left) and after 15 min (Right) of cytoplasmic dialysis of internal solution containing 0.1 mM EGTA (A) or 2 mM EGTA (B). ( $n = 5$  cells from 5 CCI mice for 0.1 mM EGTA and  $n = 5$  cells from 3 CCI mice for 2 mM EGTA). \* $P$ -value = 0.0178 compares 0.1 mM EGTA (15 min) and 2 mM EGTA (15 min); # $P$ -value = 0.0403 compares 2 mM EGTA (0 min) and 2 mM EGTA (15 min), two-way ANOVA, Dunnett's multiple comparisons test. (D) Left, fluorescent in situ hybridization of transverse lumbar spinal DH sections from male mice (white outline) showing *Pvalb* (red), *Vgat* mRNA (*Slc32a1*, yellow), SK2 mRNA (*Kcnn2*, green), and SK3 mRNA (*Kcnn3*, cyan) colocalization. Right, zoomed-in section from the yellow box on the Left shows white arrows indicating inhibitory PVNs colocalizing with *Kcnn2*. (Scale bar, 100  $\mu$ m, 50  $\mu$ m.) (E) Quantification of (D) indicating inhibitory PVNs have a higher expression of *Kcnn2* [ $273.5 \pm 7.745$  Intensity arbitrary units of measure (AUM)] than *Kcnn3* [ $130.9 \pm 2.722$  Intensity AUM]. Total of 684 VGAT+/PV+ cells counted in three mice, \*\*\*\* $P$ -value < 0.0001 paired  $t$  test. (F and G) Whole-cell current clamp representative traces (F) and mean  $\pm$  SEM of PVNs spike count in response to increasing step current injections (G) recorded in the lumbar DH spinal cord of naive male mice before (F, Left) and after bath application of 1-EBIO (0.3 mM) (F, Right) ( $n = 7$  cells from three mice). Spike count of PVNs from CCI mice shown in the dotted line for comparison but was not used in statistics. \*\* $P$ -value = 0.0021, two-way ANOVA, Šidák's multiple comparisons test. (H and I) Same as (F and G) in PVNs of CCI male mice before (H, Left) and after bath application of apamin (200 nM) (I, Right). ( $n = 8$  cells from 6 CCI mice). n.s. nonstatistically significant between naive PVNs and CCI + apamin. \* $P$ -value < 0.033 comparing naive and CCI PVNs, n.s. nonstatistically significant between naive PVNs and CCI + apamin. (J and K) Same as (F and G) in PVNs of CCI male mice before (J, Left) and after bath application of Lei-Dab7 (100 nM) (J, Right) ( $n = 8$  cells from 4 CCI mice). \* $P$ -value < 0.033 comparing naive and CCI PVNs, n.s. nonstatistically significant between naive PVNs and CCI + Lei-Dab7. (L) Mechanical sensitivity timeline of downregulation of SK2 channels in PVNs after nerve injury. (M) Baseline mechanical sensitivity was measured before CCI surgery at week 0. After verifying mechanical sensitivity is present at 28 d post-CCI (week 4, W4, gray bars), mice were injected with either the NT control ( $n = 11$ ) or the shKcnn2 ( $n = 8$ ) and tested again 2 wk after injection (week 6, W6, blue bars) (Right). The downregulation of *Kcnn2* was verified by RT-qPCR of cerebellum tissue in intracerebellar injected PV<sup>Cre</sup>; RCF tdTomato mice ( $50.48 \pm 6.1\%$  NT,  $33.32 \pm 4.3\%$  shKcnn2 normalized to Tbp, \* $P$ -value = 0.041, unpaired  $t$  test,  $n = 3$  mice per condition). Both male and female mice were used.

compared to PVNs of naive mice, the spike count of PVNs from nerve-injured mice was significantly lower. However, after PVNs of nerve-injured mice were exposed to Lei-Dab7, this significant difference was lost (Fig. 4K). The resting membrane potential and spike threshold of DH PVNs generally remained unchanged after these pharmacological applications, except for a slight increase in spike threshold after 1-EBIO application and a hyperpolarizing shift in resting membrane potential after apamin application (SI Appendix, Fig. S7 C–G). Our results demonstrate that PVNs are equipped with the conductances required for frequency adaptation but prevent their activation presumably by avoiding calcium accumulation. After nerve injury, these SK channels become activated and induce frequency adaptation, leading to a decrease in PVN output and mechanical allodynia. Consequently, blocking these SK channels in PVNs could increase their inhibitory output and alleviate mechanical allodynia. To test this hypothesis, we initially performed intrathecal injections of Lei-Dab7 in CCI mice. Given the high expression of these SK2 channels in multiple clusters of spinal cord interneurons (47), presumably also in motor interneurons, mice developed motor deficits that prevented a proper interpretation of the data. Thus, we used the PV<sup>Cre</sup>;RCF tdTOM mice and injected them intraspinally with an AAV expressing Cre-dependent FlpO and a Cre-dependent shRNA (with a floxed stop cassette inserted in the U6 promoter) against *Kcnn2* (termed shKcnn2) or a nontargeting (NT) control. This approach allowed us to reduce *Kcnn2* expression only in DH PVNs and avoid motor side effects. Our results indicate that reducing SK2 levels in PVNs of CCI mice significantly alleviates mechanical allodynia (Fig. 4L and M). Taken together, our results demonstrate that the SK2 channels present in PVNs become functionally active after nerve injury and directly contribute to mechanical allodynia.

To assess the translational potential of those observations, we set out to determine whether PVNs of the human spinal cord have a distribution similar to that seen in mice. Spinal cord segments from three male donors with no history of chronic pain (average age: 53; SI Appendix, Table S3) were used ISH experiments. *PVALB* expression was found in both the human dorsal and ventral horns. Within the human DH, the distribution of *PVALB*-positive cells was similar to that observed in C57BL/6 male mice (SI Appendix, Fig. S8). Further studies will be required to determine whether human spinal PVNs change their firing pattern after nerve injury.

## Discussion

Chronic neuropathic pain is a debilitating condition for which new treatment approaches are needed. The condition manifests itself after nerve injury and persists long after the injury has subsided (1). One of the hallmarks of neuropathic pain is mechanical allodynia, where gentle light touch stimuli are perceived as painful. It is widely accepted that chronic neuropathic pain is due in part to a decreased inhibitory tone in the DH of the spinal cord (2–4, 48). One subset of spinal inhibitory neurons that recently received attention for its role in mechanical allodynia after nerve injury is the PVNs. In models of autism, where a hypofunction of PVNs has been established (11–16), such decreased inhibitory output has been proposed to result from reductions in PV protein expression, loss of PVNs, or reductions in their fast spiking behaviors (11). In the spinal cord, recent reports suggest that PVNs become hypofunctional after nerve injury (6, 10, 21, 44), which would enable touch-sensitive A $\beta$  fibers to activate pain-processing spinal circuits. However, the mechanisms responsible for this decreased activity of spinal PVNs remain unknown.

We propose that the loss of inhibitory output from PVNs after peripheral nerve injury could be due to at least three mechanisms.

The efficacy of their synaptic connection with their targets could be reduced, through pruning of their terminals, decreased vesicular content of their inhibitory transmitters, or decreased postsynaptic receptors. A second possibility could be the decreased excitatory drive onto PVNs from peripheral A $\beta$  fibers. It was reported that after nerve injury, the amplitude of A $\beta$ -fiber stimulated excitatory postsynaptic potentials recorded in lamina III glycinergic neurons (characteristic of PVNs) was decreased and increased the failure rate to generate action potentials (49). This suggests an increase in the failure rate of synaptic transmission between A $\beta$  and inhibitory PVNs after peripheral nerve injury. Further experiments such as recording from PVNs and PKC $\gamma$  neurons while stimulating A $\beta$  fibers are required to properly test these hypotheses.

A third possibility for the reduced inhibitory output of PVNs after nerve injury is a change in their intrinsic electrical properties. We speculated that if a reduced A $\beta$  input alone was responsible for the decreased activity of PVNs after nerve injury, we should be able to directly stimulate the soma of these PVNs and observe a firing pattern similar to naive mice. However, our results indicate that PVNs from nerve-injured mice respond differently to the injection of depolarizing currents. Indeed, after nerve injury, the hypofunction of PVNs manifests itself as a change in their firing pattern, in which they switch from a tonic firing to an adaptive firing mode. This would have a dramatic impact on their output as they would not be able to prevent A $\beta$  inputs from activating a polysynaptic pathway that results in mechanical allodynia (Fig. 5). We modeled this possibility in a recent computational study (44), in which we showed that after nerve injury PVNs have a reduced firing activity, which can no longer prevent the activation of PKC $\gamma$  neurons by A $\beta$  fibers. The spike frequency adaptation that we observe suggests that nerve injury recruits calcium-activated potassium conductances. The increased contribution of these channels is presumably the result of 1) impaired calcium buffering caused by the decrease in PV expression after nerve injury and 2) the proximity between voltage-gated calcium channels and SK channels, as evidence for such spatial and functional coupling of calcium entry sites and effector mechanisms has previously been demonstrated in other CNS regions (50, 51). Interestingly, a decrease in PV expression has also been shown in a rat model of acute knee inflammation, in which PV expression decreased slightly but significantly 28 h after the inflammation (52).

It is unclear the extent to which each of these three mechanisms contribute to the hypofunction of DH PVNs and which mechanism should be targeted for therapeutic pain relief. We demonstrated that the adaptive firing observed in PVNs of nerve-injured mice could be reversed by blocking SK2 channels, confirming their role in this phenomenon. Furthermore, down-regulating SK2 channels in PVNs significantly alleviated mechanical allodynia in nerve-injured mice. However, the restoration of PV expression in PVNs was able to prevent, but not alleviate injury-induced allodynia, indicating that nerve injury likely recruits additional mechanisms that ultimately govern the output of PVNs.

The model presented here describes how this DH circuit functions under naive conditions and proposes an intrinsic molecular mechanism responsible for the decreased inhibitory tone in PVNs after nerve injury. However, it will almost certainly require revision as these, and other data become available. We have depicted the model with PKC $\gamma$  neurons as the postsynaptic targets of PVNs, but these constitute only 20% of the targets of PVNs and a similar inhibitory mechanism may apply to other excitatory neurons. The model is, however, consistent with available data, and it serves as a useful framework for designing future experiments. For instance, it is noteworthy that the firing pattern of PVNs from shPvalb-injected healthy mice does not exactly resemble that of PVNs from nerve-injured mice, suggesting that additional mechanisms affecting

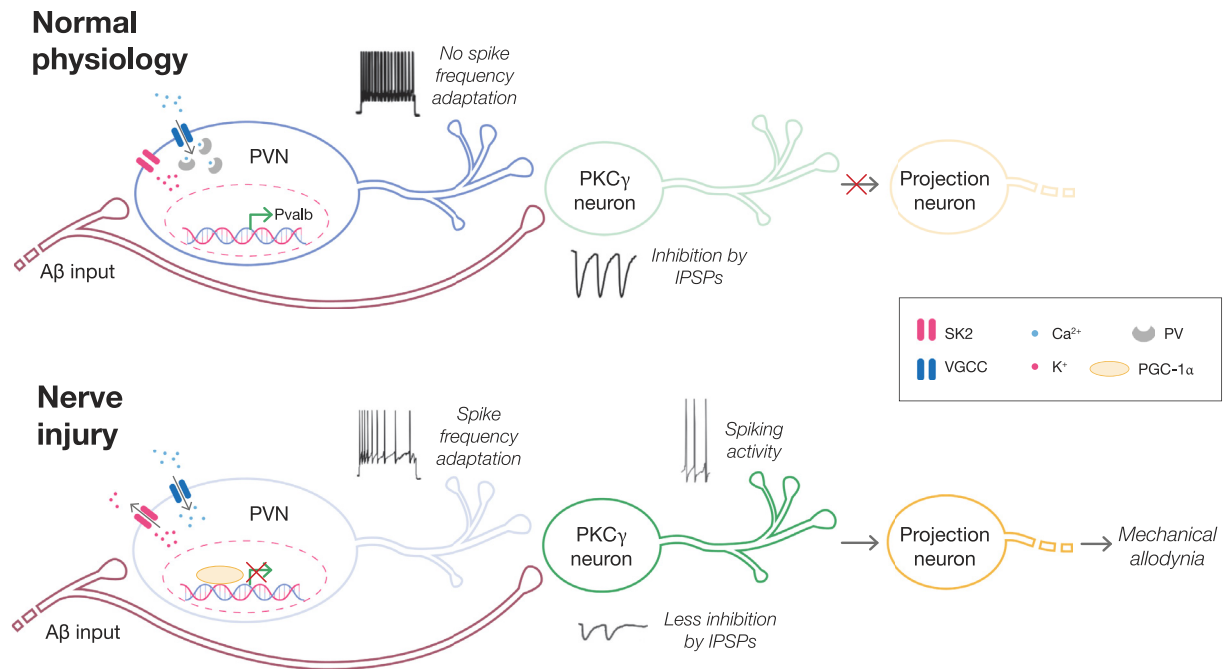


**Fig. 5.** General organization of PVN and PKC $\gamma$  neuron relationship in normal and neuropathic pain conditions. Under naive conditions, PV in the PVNs chelates the free intracellular calcium ions, thereby inhibiting the activation of SK2 channels and preventing the influx of K<sup>+</sup> ions. No PVN spike frequency adaptation occurs which allows for inhibition of the polysynaptic pathway links between A $\beta$  fibers to lamina I projection neurons. After nerve injury, a decrease in PV concentration results in an increase of the free intracellular calcium and activation of SK2 channels that allow for spike frequency adaptation of PVNs to appear. This adaptation decreases their inhibition on PKC $\gamma$  neurons enabling low-threshold inputs to drive lamina I projection neurons and causes mechanical allodynia.

PVN excitability are likely recruited by nerve injury. Furthermore, studies of cerebellar PVNs synapsing on Purkinje cells have shown that in PV knockout mice, the absence of PV could change a depressing synapse into a facilitating one, likely through the accumulation of calcium at the terminal (53). Another study in these knockout mice suggested that inhibitory postsynaptic currents from hippocampal PVNs onto pyramidal cells could be facilitated by trains of stimuli at frequencies over 20 Hz (54). If one omits the general concerns associated with compensatory changes associated with embryonic knockout models, these studies suggest that should inputs arrive at PVNs terminal at high frequencies, they will result in larger quantal release or greater postsynaptic inhibition. However, when we reduce the expression of PV in spinal or hippocampal PVNs of wild-type mice, the excitability profile changes in such a drastic manner that the neurons are not able to sustain high firing frequencies for very long. They rapidly undergo spike frequency adaptation and are unable to emit any action potential. Furthermore, recordings from postsynaptic targets of DH PVNs have demonstrated a reduced inhibitory potential after nerve injury (21).

In conclusion, we propose a model in which the incoming inputs from A $\beta$  fibers are prevented from polysynaptically activating lamina I projection neurons because PVNs receive a copy of this input and impose it on their postsynaptic targets, whether these are PKC $\gamma$  neurons (5, 21, 55), vertical cells (6), or the central terminals of A $\beta$  fibers themselves (6, 7, 56). Such a forward inhibitory mechanism is only possible if the firing pattern of PVNs can match exactly the continuous firing pattern of the A $\beta$  fibers. If PVNs develop frequency adaptation, they will not efficiently prevent the activation of their targets, which will initiate the polysynaptic activation of lamina I projection neurons involved in pain signaling. Approaches aimed at increasing the excitability of PVNs may therefore have therapeutic potential and should thus be further investigated.

## Materials and Methods

**Experimental Animals and Subject Details.***Mice.* Male mice (8 to 14 wk old) were kept on a 12-h:12-h light/dark cycle, with food and water provided ad libitum. All experimental procedures were approved by the Animal Care and Use Committee at McGill University, in accordance with the regulations of the Canadian Council on Animal Care. All mouse strains have previously been described. PV<sup>Cre</sup>, B6 PV<sup>Cre</sup>, Pvalb-tdTomato, PV<sup>Cre</sup>-tdTom reporter, Ai65F (RCF tdTom), and Pv-CreERT2 (PV KO) were obtained from The Jackson Laboratory (Catalog #008069, #017320, #027395, #007914, #032864, and #010777, respectively). C57BL/6 mice aged 8 to 12 wk were purchased from Charles Rivers.

**Generation of PV<sup>Cre</sup>; RCF tdTomato Mice for Slice Electrophysiology.** A PV<sup>Cre</sup> mouse expressing Cre recombinase in Pvalb-expressing neurons was crossed with an RCF-tdTomato mouse expressing *flr*-flanked STOP cassette preventing the transcription of tdTomato fluorescent protein. The offspring was intraspinally injected with an AAV containing Cre-dependent FLPo. Only PVNs infected with FLPo are tdTomato-positive and suitable for electrophysiology recordings.

**Humans.** Lumbar spinal cords were sourced from anonymized organ donors (all demographic data are listed in *SI Appendix, Table S3*), confirmed neurologically deceased, in compliance with protocols sanctioned by the French organ transplantation authority, Agence de la Biomédecine."

See *SI Appendix, Methods and Materials* for details on in situ hybridization, quantitative PCR, immunohistochemistry, AAV virus production, microscopy and image analysis, virus injection surgeries, behavior, and electrophysiology.

**Illustrations.** All figures presented in this manuscript were assembled in CorelDRAW Graphic Suite. Fig. 5 was designed by Owain Roberts.

**Statistics.** All statistical analyses were performed using GraphPad Prism v9.3.0 software, and individual test names are indicated in figure legends. Data were presented as mean  $\pm$  SEM. A *P*-value of *P* < 0.05 was the criterion for significance. n.s. was denoted as not statistically significant.

**Data, Materials, and Software Availability.** All study data are included in the article and/or *SI Appendix*.

**ACKNOWLEDGMENTS.** We gratefully acknowledge the gift of human tissue from the donors included in this work and their families. Images used for

this manuscript were collected in the McGill University Advanced Biomedicine Facility, (RRID:SCR\_017697), Institut de Recherches Cliniques de Montréal Microscopy and Imaging Platform, and the Montpellier Imaging Platform. We are thankful to Ms. Tanya Koch at the McGill University Comparative Medicine and Animal Resources Centre for the mice colony management. We thank Dr. Magali Millecamps and the McGill Animal Behavioural Characterization platform for the mouse behavior experimental support. We thank Dr. Theodore

Price for providing access to the human DH reference atlas. H.Q. was funded over different periods by a Canadian Institutes of Health Research (CIHR) Master's fellowship, the Edwards Ph.D. Studentship in Pain Research, and the Healthy Brains Healthy Lives PhD fellowship. E.B. was supported by the LABEX Ion Channels Science and Therapeutics Agence Nationale de la Recherche grant. R.S.-N. was supported by a project grant from the CIHR PJT-162404.

1. M. P. Jensen, M. J. Chodroff, R. H. Dworkin, The impact of neuropathic pain on health-related quality of life: Review and implications. *Neurology* **68**, 1178–1182 (2007).
2. J. M. Castro-Lopes, I. Tavares, A. Coimbra, GABA decreases in the spinal cord dorsal horn after peripheral neurectomy. *Brain Res.* **620**, 287–291 (1993).
3. J. A. M. Coull *et al.*, Trans-synaptic shift in anion gradient in spinal lamina I neurons as a mechanism of neuropathic pain. *Nature* **424**, 938–942 (2003).
4. K. A. Moore *et al.*, Partial peripheral nerve injury promotes a selective loss of GABAergic inhibition in the superficial dorsal horn of the spinal cord. *J. Neurosci.* **22**, 6724–6731 (2002).
5. H. Petitjean *et al.*, Dorsal horn parvalbumin neurons are gate-keepers of touch-evoked pain after nerve injury. *Cell Rep.* **13**, 1246–1257 (2015).
6. K. A. Boyle *et al.*, Defining a spinal microcircuit that gates myelinated afferent input: Implications for tactile allodynia. *Cell Rep.* **28**, 526–540.e6 (2019).
7. D. I. Hughes, S. Sikander, C. M. Kinnon, Morphological, neurochemical and electrophysiological features of parvalbumin-expressing cells: A likely source of axo-axonic inputs in the mouse spinal dorsal horn. *J. Physiol.* **590**, 3927–3951 (2012).
8. E. Foster *et al.*, Targeted ablation, silencing, and activation establish glycinergic dorsal horn neurons as key components of a spinal gate for pain and itch. *Neuron* **85**, 1289–1304 (2015).
9. M. A. Gradwell *et al.*, Diversity of inhibitory and excitatory parvalbumin interneuron circuits in the dorsal horn. *Pain* **163**, e432 (2022).
10. G. Rankin *et al.*, Nerve injury disrupts temporal processing in the spinal cord dorsal horn through alterations in PV+ interneurons. *Cell Rep.* **43**, 113718 (2024).
11. A. Contractor, I. M. Ethell, C. Portera-Cailliau, Cortical interneurons in autism. *Nat. Neurosci.* **24**, 1648–1659 (2021).
12. O. Marin, Interneuron dysfunction in psychiatric disorders. *Nat. Rev. Neurosci.* **13**, 107–120 (2012).
13. B. R. Ferguson, W.-J. Gao, PV interneurons: Critical regulators of E/I balance for prefrontal cortex-dependent behavior and psychiatric disorders. *Front. Neural Circuits* **12**, 37 (2018).
14. F. Filice, L. Janickova, T. Henzi, A. Bilella, B. Schwaller, The parvalbumin hypothesis of autism spectrum disorder. *Front. Cell. Neurosci.* **14**, 577525 (2020).
15. J. W. Lunden, M. Durens, A. W. Phillips, M. W. Nestor, Cortical interneuron function in autism spectrum condition. *Pediatr. Res.* **85**, 146–154 (2019).
16. E. Rossignol, Genetics and function of neocortical GABAergic interneurons in neurodevelopmental disorders. *Neural Plast.* **2011**, 649325 (2011).
17. A. H. Meyer, I. Katona, M. Blatov, A. Rozov, H. Monyer, In vivo labeling of parvalbumin-positive interneurons and analysis of electrical coupling in identified neurons. *J. Neurosci.* **22**, 7055–7064 (2002).
18. Z. G. Piao *et al.*, Activation of glia and microglial p38 MAPK in medullary dorsal horn contributes to tactile hypersensitivity following trigeminal sensory nerve injury. *Pain* **121**, 219–231 (2006).
19. M. Häring *et al.*, Neuronal atlas of the dorsal horn defines its architecture and links sensory input to transcriptional cell types. *Nat. Neurosci.* **21**, 869–880 (2018).
20. U. Blömer *et al.*, Highly efficient and sustained gene transfer in adult neurons with a lentivirus vector. *J. Virol.* **71**, 6641–6649 (1997).
21. B. Cao, G. Scherrer, L. Chen, Spinal cord retinoic acid receptor signaling gates mechanical hypersensitivity in neuropathic pain. *Neuron* **110**, 4108–4124.e6 (2022).
22. J. M. Braz, B. Rico, A. I. Basbaum, Transneuronal tracing of diverse CNS circuits by Cre-mediated induction of wheat germ agglutinin in transgenic mice. *Proc. Natl. Acad. Sci. U.S.A.* **99**, 15148–15153 (2002).
23. C. Peirs *et al.*, Dorsal horn circuits for persistent mechanical pain. *Neuron* **87**, 797–812 (2015).
24. A. Francois *et al.*, A brainstem-spinal cord inhibitory circuit for mechanical pain modulation by GABA and Enkephalins. *Neuron* **93**, 822–839.e6 (2017).
25. A. B. Malmberg, C. Chen, S. Tonegawa, A. I. Basbaum, Preserved acute pain and reduced neuropathic pain in mice lacking PKCγ. *Science* **278**, 279–283 (1997).
26. L. S. Miraucourt, R. Dallel, D. L. Voisin, Glycine inhibitory dysfunction turns touch into pain through PKCγ interneurons. *PLoS One* **2**, e1116 (2007).
27. D. Mochly-Rosen, A. S. Gordon, Anchoring proteins for protein kinase C: A means for isozyme selectivity. *FASEB J.* **12**, 35–42 (1998).
28. J.-M. Zhang, J. An, Cytokines, inflammation, and pain. *Int. Anesthesiol. Clin.* **45**, 27–37 (2007).
29. S. Nadeau *et al.*, Functional recovery after peripheral nerve injury is dependent on the pro-inflammatory cytokines IL-1β and TNF: Implications for neuropathic pain. *J. Neurosci.* **31**, 12533–12542 (2011).
30. D. Schomberg, M. Ahmed, G. Miranpuri, J. Olson, D. K. Resnick, Neuropathic pain: Role of inflammation, immune response, and ion channel activity in central injury mechanisms. *Ann. Neurosci.* **19**, 125–132 (2012).
31. E. K. Lucas *et al.*, Parvalbumin deficiency and GABAergic dysfunction in mice lacking PGC-1α. *J. Neurosci.* **30**, 7227–7235 (2010).
32. E. K. Lucas *et al.*, PGC-1α provides a transcriptional framework for synchronous neurotransmitter release from parvalbumin-positive interneurons. *J. Neurosci.* **34**, 14375–14387 (2014).
33. H.-J. Kim *et al.*, Effects of PGC-1α on TNF-α-induced MCP-1 and VCAM-1 expression and NF-κB activation in human aortic smooth muscle and endothelial cells. *Antioxid. Redox Signal.* **9**, 301–307 (2007).
34. X. Yang, S. Xu, Y. Qian, Q. Xiao, Resveratrol regulates microglia M1/M2 polarization via PGC-1α in conditions of neuroinflammatory injury. *Brain Behav. Immun.* **64**, 162–172 (2017).
35. Y. Gao *et al.*, PARP-1-regulated TNF-α expression in the dorsal root ganglia and spinal dorsal horn contributes to the pathogenesis of neuropathic pain in rats. *Brain Behav. Immun.* **88**, 482–496 (2020).
36. M. Bartos, I. Vida, P. Jonas, Synaptic mechanisms of synchronized gamma oscillations in inhibitory interneuron networks. *Nat. Rev. Neurosci.* **8**, 45–56 (2007).
37. F. C. Roth, H. Hu, An axon-specific expression of HCN channels catalyzes fast action potential signaling in GABAergic interneurons. *Nat. Commun.* **11**, 1–10 (2020).
38. D. I. Hughes *et al.*, HCN4 subunit expression in fast-spiking interneurons of the rat spinal cord and hippocampus. *Neuroscience* **237**, 7–18 (2013).
39. S. R. Chaplan *et al.*, Neuronal hyperpolarization-activated pacemaker channels drive neuropathic pain. *J. Neurosci.* **23**, 1169–1178 (2003).
40. H. Tu *et al.*, The effects of intrathecal application of ZD7288, and HCN blocker, on mechanical allodynia of neuropathic pain model rats. *Chin. J. Pain Med.* **12**, 228–233 (2006).
41. S.-H. Lee, B. Schwaller, E. Neher, Kinetics of Ca<sup>2+</sup> binding to parvalbumin in bovine chromaffin cells: Implications for [Ca<sup>2+</sup>]<sub>i</sub> transients of neuronal dendrites. *J. Physiol.* **525**, 419–432 (2000).
42. B. Schwaller, Cytosolic Ca<sup>2+</sup> buffers are inherently Ca<sup>2+</sup> signal modulators. *Cold Spring Harb. Perspect. Biol.* **12**, a035543 (2020).
43. D. Orduz, D. P. Biscop, B. Schwaller, S. N. Schiffmann, D. Gall, Parvalbumin tunes spike-timing and efferent short-term plasticity in striatal fast spiking interneurons. *J. Physiol.* **591**, 3215–3232 (2013).
44. X. Ma, L. S. Miraucourt, H. Qiu, R. Sharif-Naeini, A. Khadra, Modulation of SK channels via calcium buffering tunes intrinsic excitability of parvalbumin interneurons in neuropathic pain: A computational and experimental investigation. *J. Neurosci.* **43**, 5608–5622 (2023).
45. X. Li, D. J. Bennett, Apamin-sensitive calcium-activated potassium currents (SK) are activated by persistent calcium currents in rat motoneurons. *J. Neurophysiol.* **97**, 3314–3330 (2007).
46. V. G. Shakkottai *et al.*, Design and characterization of a highly selective peptide inhibitor of the small conductance calcium-activated K<sup>+</sup> channel, SKCa2. *J. Biol. Chem.* **276**, 43145–43151 (2001).
47. D. E. Russ *et al.*, A harmonized atlas of mouse spinal cord cell types and their spatial organization. *Nat. Commun.* **12**, 5722 (2021).
48. I. Lever, J. Cunningham, J. Grist, P. K. Yip, M. Malcangio, Release of BDNF and GABA in the dorsal horn of neuropathic rats. *Eur. J. Neurosci.* **18**, 1169–1174 (2003).
49. Y. Lu *et al.*, A feed-forward spinal cord glycinergic neural circuit gates mechanical allodynia. *J. Clin. Invest.* **123**, 4050–4062 (2013).
50. S. Kakizawa *et al.*, Junctophilin-mediated channel crosstalk essential for cerebellar synaptic plasticity. *EMBO J.* **26**, 1924–1933 (2007).
51. B. Fakler, J. P. Adelman, Control of K(Ca) channels by calcium nano/microdomains. *Neuron* **59**, 873–881 (2008).
52. G. Zacharova, D. Sojka, J. Palecek, Changes of parvalbumin expression in the spinal cord after peripheral inflammation. *Physiol. Res.* **58**, 435–442 (2009).
53. O. Caillard *et al.*, Role of the calcium-binding protein parvalbumin in short-term synaptic plasticity. *Proc. Natl. Acad. Sci. U.S.A.* **97**, 13372–13377 (2000).
54. M. Vreugdenhil, J. G. R. Jefferys, M. R. Celio, B. Schwaller, Parvalbumin-deficiency facilitates repetitive IPSCs and gamma oscillations in the hippocampus. *J. Neurophysiol.* **89**, 1414–1422 (2003).
55. L. Medlock *et al.*, Multiscale computer model of the spinal dorsal horn reveals changes in network processing associated with chronic pain. *J. Neurosci.* **42**, 3133–3149 (2022).
56. V. E. Abraira *et al.*, The cellular and synaptic architecture of the mechanosensory dorsal horn. *Cell* **168**, 295–310.e19 (2017).